
This copy is for your personal, non-commercial use only.

If you wish to distribute this article to others, you can order high-quality copies for your colleagues, clients, or customers by [clicking here](#).

Permission to republish or repurpose articles or portions of articles can be obtained by following the guidelines [here](#).

The following resources related to this article are available online at www.sciencemag.org (this information is current as of August 25, 2014):

Updated information and services, including high-resolution figures, can be found in the online version of this article at:

<http://www.sciencemag.org/content/288/5463/113.full.html>

This article **cites 34 articles**, 6 of which can be accessed free:

<http://www.sciencemag.org/content/288/5463/113.full.html#ref-list-1>

This article has been **cited by** 868 article(s) on the ISI Web of Science

This article has been **cited by** 72 articles hosted by HighWire Press; see:

<http://www.sciencemag.org/content/288/5463/113.full.html#related-urls>

This article appears in the following **subject collections**:

Physics, Applied

http://www.sciencemag.org/cgi/collection/app_physics

Monolithic Microfabricated Valves and Pumps by Multilayer Soft Lithography

Marc A. Unger, Hou-Pu Chou, Todd Thorsen, Axel Scherer, Stephen R. Quake*

Soft lithography is an alternative to silicon-based micromachining that uses replica molding of nontraditional elastomeric materials to fabricate stamps and microfluidic channels. We describe here an extension to the soft lithography paradigm, multilayer soft lithography, with which devices consisting of multiple layers may be fabricated from soft materials. We used this technique to build active microfluidic systems containing on-off valves, switching valves, and pumps entirely out of elastomer. The softness of these materials allows the device areas to be reduced by more than two orders of magnitude compared with silicon-based devices. The other advantages of soft lithography, such as rapid prototyping, ease of fabrication, and biocompatibility, are retained.

The application of micromachining techniques is growing rapidly, driven by the dramatic success of a few key applications such as microfabricated accelerometers (1, 2), pressure sensors (3), and ink-jet print heads (4). New applications are appearing in other fields, in particular fiber optic communications (5, 6), displays (7), and microfluidics (8–12). The two most widespread methods for the production of microelectromechanical structures (MEMS) are bulk micromachining and surface micromachining. Bulk micromachining is a subtractive fabrication method whereby single-crystal silicon is lithographically patterned and then etched to form three-dimensional (3D) structures. Surface micromachining, in contrast, is an additive method where layers of semiconductor-type materials (polysilicon, metals, silicon nitride, silicon dioxide, and so forth) are sequentially added and patterned to make 3D structures.

Bulk and surface micromachining methods are limited by the materials used. The semiconductor-type materials typically used in bulk and surface micromachining are stiff materials with Young's modulus ~ 100 GPa (13). Because the forces generated by micromachined actuators are limited, the stiffness of the materials limits the minimum size of many devices. Furthermore, because multiple layers must be built up to make active devices, adhesion between layers is a problem of great practical concern. For bulk micromachining, wafer-bonding techniques must be used to create multilayer structures. For surface micromachining, thermal stress between layers limits the total device thickness to ~ 20 μm . Clean-room fabrication and careful con-

trol of process conditions are required to realize acceptable device yields.

An alternative microfabrication technique based on replication molding is gaining popularity. Typically, an elastomer is patterned by curing on a micromachined mold. Loosely termed soft lithography, this technique has been used to make blazed grating optics (14), stamps for chemical patterning (15), and microfluidic devices (16–20). Soft lithography's advantages include the capacity for rapid prototyping, easy fabrication without expensive capital equipment, and forgiving process parameters. For applications with moderate-sized features (≥ 20 μm) such as microfluidics, molds can be patterned by using a high-resolution transparency film as a contact mask for a thick photoresist layer (21). A single researcher can design, print, pattern the mold, and create a new set of cast-elastomer devices within 1 day, and subsequent elastomer casts can be made in just a few hours. The tolerant process parameters for elastomer casting allow devices to be produced in ambient laboratory conditions instead of a clean room. However, soft lithography also has limitations: It is fundamentally a subtractive method (in the sense that the mold defines where elastomer is removed), and with only one elastomer layer it is difficult to create active devices or moving parts. A method for bonding elastomer components by plasma oxidation has been described previously (21) and has been used to seal microfluidic channels against flat elastomer substrates (20, 22).

We describe here a technique called "multilayer soft lithography" that combines soft lithography with the capability to bond multiple patterned layers of elastomer. Multilayer structures are constructed by bonding layers of elastomer, each of which is separately cast from a micromachined mold (Fig. 1A). The elastomer is a two-component addition-cure

silicone rubber. The bottom layer has an excess of one of the components (A), whereas the upper layer has an excess of the other (B). After separate curing of the layers, the upper layer is removed from its mold and placed on top of the lower layer, where it forms a hermetic seal. Because each layer has an excess of one of the two components, reactive molecules remain at the interface between the layers. Further curing causes the two layers to irreversibly bond: The strength of the interface equals the strength of the bulk elastomer. This process creates a monolithic three-dimensionally patterned structure composed entirely of elastomer. Additional layers are added by simply repeating the process: Each time the device is sealed on a layer of opposite "polarity" (A versus B) and cured, another layer is added.

The ease of producing multilayers makes it possible to have multiple layers of fluidics, a difficult task with conventional micromachining. We created test structures of up to seven patterned layers in this fashion (23), each of ~ 40 μm thickness (Fig. 2F). Because the devices are monolithic (i.e., all of the layers are composed of the same material), interlayer adhesion failures and thermal stress problems are completely avoided. Particulates disturb interlayer adhesion very little, if at all. Perhaps most importantly for the actuation of microstructures, the elastomer is a soft material with Young's modulus (24) ~ 750 kPa, allowing large deflections with small actuation forces. One can also control the physical properties of the material. We created magnetic layers of elastomer by adding fine iron powder and electrically conducting layers by doping with carbon black above the percolation threshold (25). There is thus the possibility of creating all-elastomer electro-magnetic devices (26).

To demonstrate the power of multilayer soft lithography, we fabricated active valves and pumps. Monolithic elastomeric valves and pumps, like other mechanical microfluidic devices, avoid several practical problems affecting flow systems based on electroosmotic flow (8, 9, 20, 27–29) or dielectrophoresis (30, 31), such as electrolytic bubble formation around the electrodes and a strong dependence of flow on the composition of the flow medium (32–34). Electrolytic bubble formation, although not a problem for laboratory devices, seriously restricts the use of electroosmotic flow in integrated microfluidic devices. Also, neither electroosmotic nor dielectrophoretic flow can easily be used to stop flow or balance pressure differences.

We fabricated our valves using a crossed-channel architecture (Fig. 1A). Typical channels are 100 μm wide and 10 μm high, making the active area of the valve 100 μm by 100 μm . The membrane of polymer between the channels is engineered to be rela-

Department of Applied Physics, California Institute of Technology, Pasadena, CA 91125, USA.

*To whom correspondence should be addressed. E-mail: quake@caltech.edu

REPORTS

tively thin (typically 30 μm). When pressure is applied to the upper channel ("control channel"), the membrane deflects downward. Sufficient pressure closes the lower channel ("flow channel"). For optical convenience, we typically seal our structures with glass as

the bottom layer; this bond with glass is reversible, so devices may be peeled up, washed, and reused. We also fabricated devices where the bottom layer is another layer of elastomer, which is useful when higher back pressures are used. The response time of

devices actuated in this fashion is on the order of 1 ms, and the applied pressures are on the order of 100 kPa, so a 100 μm by 100 μm area gives actuation forces on the order of 1 mN. Pneumatic actuation allows active devices to be densely packed; we built microfluidics with densities of 30 devices per square millimeter, and greater densities are achievable. This actuation speed, pressure, and device density are more than adequate for the vast majority of microfluidic applications.

The shape of the flow channel is important for proper actuation of the valve (Fig. 1B). Rectangular and even trapezoidal shaped channels will not close completely under pressure from above. Flow channels with a round cross section close completely; the round shape transfers force from above to the channel edges and causes the channel to close from edges to center. We found that 100 μm by 100 μm by 10 μm valves over trapezoidal channels would not close completely even at 200 kPa of applied pressure, whereas rounded channels sealed completely at only 40 kPa.

Making multiple, independently actuated valves in one device simply requires independent control of the pressure applied to each control line (35). Figure 2, A to E, shows simple configurations resulting in on-off valves (Fig. 2, A and B), a pump (Fig. 2C), a grid of valves (Fig. 2D), and a switching valve (Fig. 2E). Each control line can actuate multiple valves simultaneously. Because the width of the control lines can be varied and membrane deflection depends strongly on membrane dimensions, it is possible to have a control line pass over multiple flow channels and actuate only the desired ones. The active element is the roof of the channel itself, so simple on-off valves (and pumps) produced by this technique have truly zero dead volume; switching valves have a dead volume about equal to the active volume of one valve, that is, 100 μm \times 100 μm \times 10 μm = 100 pl. The dead volume required and the area consumed by the moving membrane are each about two orders of magnitude smaller than any microvalve demonstrated to date (11).

The valve opening can be precisely controlled by varying the pressure applied to the control line. As demonstrated in Fig. 3A, the response of the valve is almost perfectly linear over a large portion of its range of travel, with minimal hysteresis. Thus, these valves can be used for microfluidic metering and flow control. The linearity of the valve response demonstrates that the individual valves are well-modeled as Hooke's law springs. Furthermore, high pressures in the flow channel ("back pressure") can be countered simply by increasing the actuation pressure. Within the experimental range we were able to test (up to 70-kPa back pressure), valve closing was achieved by simply adding the

Fig. 1. (A) Process flow for multilayer soft lithography. The elastomer used here is General Electric Silicones RTV 615. Part "A" contains a polydimethylsiloxane bearing vinyl groups and a platinum catalyst; part "B" contains a cross-linker containing silicon hydride (Si-H) groups, which form a covalent bond with vinyl groups. RTV 615 is normally used at a ratio of 10 A:1 B. For bonding, one layer is made with 30 A:1 B (excess vinyl groups) and the other with 3 A:1 B (excess Si-H groups). The top layer is cast thick (~4 mm) for mechanical stability, whereas the other layers are cast thin. The thin layer was created by spin-coating the RTV mixture on a microfabricated mold at 2000 rpm for 30 s, yielding a thickness of ~40 μm . Each layer was separately baked at 80°C for 1.5 hours. The thick layer was then sealed on the thin layer, and the two were bonded at 80°C for 1.5 hours. Molds were patterned photoresist on silicon wafers. Shipley SJR 5740 photoresist was spun at 2000 rpm, patterned with a high-resolution transparency film as a mask, and developed to yield inverse channels of 10 μm in height. When baked at 200°C for 30 min, the photoresist reflows and the inverse channels become rounded. Molds were treated with trimethylchlorosilane vapor for 1 min before each use to prevent adhesion of silicone rubber. **(B)** Schematic of valve closing for square and rounded channels. The dotted lines indicate the contour of the top of the channel for rectangular (left) and rounded (right) channels as pressure is increased. Valve sealing can be inspected by observing the elastomer-substrate interface under an optical microscope: It appears as a distinct, visible edge. Incomplete sealing as with a rectangular channel appears as an "island" of contact in the flow channel; complete sealing (as observed with rounded channels) gives a continuous contact edge joining the left and right edges of the flow channel.

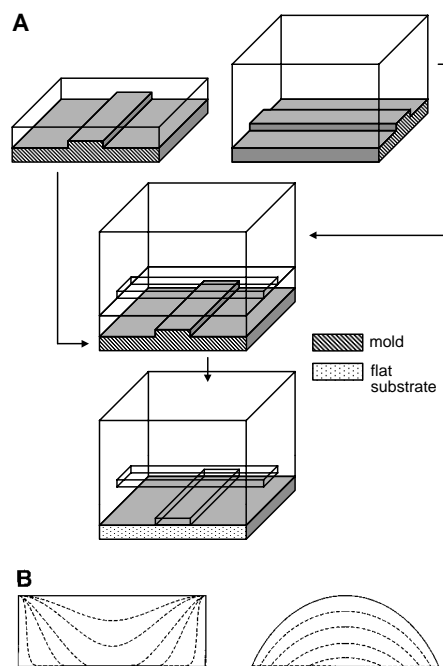
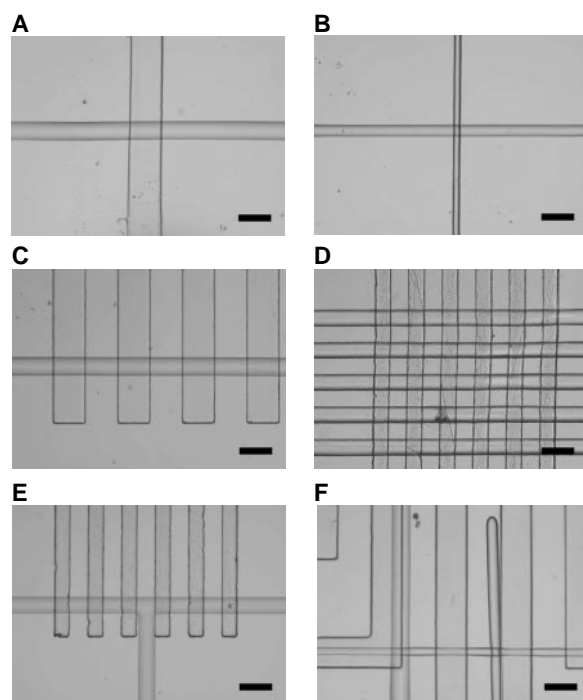


Fig. 2. Optical micrographs of different valve and pump configurations; control lines are oriented vertically. **(A)** Simple on-off valve with 200- μm control line and 100- μm flow line ("200 \times 100"). **(B)** 30 \times 50 on-off valve. **(C)** Peristaltic pump. Only three of the four control lines shown were used for actuation. **(D)** Grid of on-off valves. **(E)** Switching valve. Typically, only the innermost two control lines were used for actuation. **(F)** Section of the seven-layer test structure mentioned in the text. All scale bars are 200 μm .



REPORTS

back pressure to the minimum closing pressure at zero back pressure.

Monolithic elastomer valves fabricated as described here can be actuated with surprising speed. The time response for a valve filled with aqueous solution is on the order of 1 ms, as shown in Fig. 3B. The valve still opens and closes at 100 Hz, although it does not open completely. The valve responds nearly instantaneously to the applied pressure, but applied pressure lags substantially behind the control signal (36).

We also fabricated a peristaltic pump from three valves arranged on a single channel (Fig. 4A). Pumping rates were determined by measuring the distance traveled by a column of water in thin (0.5 mm interior diameter) tubing; with 100 μm by 100 μm by 10 μm valves, a maximum pumping rate of 2.35 nl/s was measured (Fig. 4B). Consistent with the previous observations of valve actuation speed, the maximum pumping rate is attained at ~ 75 Hz; above this rate, increasing numbers of pump cycles compete with incomplete

valve opening and closing. The pumping rate was nearly constant until above 200 Hz and fell off slowly until 300 Hz. The valves and pumps are also quite durable: We have never observed the elastomer membrane, control channels, or bond to fail. None of the valves in the peristaltic pump described above show any sign of wear or fatigue after more than 4 million actuations. In addition to their durability, they are also gentle. A solution of *Escherichia coli* pumped through a channel and tested for viability showed a 94% survival rate (37).

Monolithic active valves built as described here have several notable advantages over silicon-based microfluidic valves. Because of the low Young's modulus of silicone rubber, the valves' active area is no larger than the channels themselves; this permits exceptionally low dead volumes. Because of the softness of the membrane, complete valve sealing is easily attained, even in the presence of particulates. The valves close linearly with applied pressure, allowing metering and per-

mitting them to close in spite of high back pressure. Their small size makes them fast, and size and softness both contribute to making them durable. Small size, pneumatic actuation, and the ability to cross channels without actuating them allow a dense integration of microfluidic pumps, valves, mixing chambers, and switch valves in a single, easy-to-fabricate microfluidic chip. The greatest advantage, however, is ease of production. Compared with valves and pumps made with conventional silicon-based micromachining (11) [or even hybrid devices incorporating polymers (38–41)], monolithic elastomer valves are simpler and much easier to fabricate.

The use of nontraditional materials gives the multilayer soft lithography method a number of advantages over conventional micromachining, including rapid prototyping, ease of fabrication, and forgiving process parameters. It allows multilayer fabrication without the problems of interlayer adhesion and thermal stress buildup that are endemic to conventional micromachining. This process can be used to construct complex multilayer microfabricated structures such as optical trains and microfluidic valves and pumps. The silicone rubber used here is transparent to visible light, making optical interrogation of microfluidic devices simple. It is also biocompatible—materials in this family are used to fabricate contact lenses. The raw material is inexpensive, especially when compared

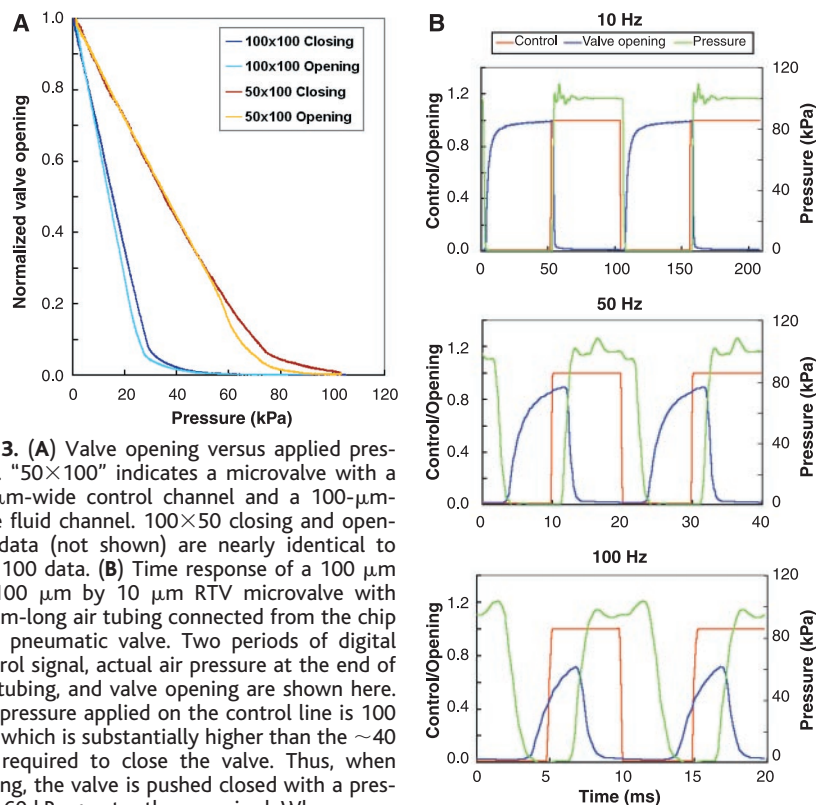


Fig. 3. (A) Valve opening versus applied pressure. "50 \times 100" indicates a microvalve with a 50- μm -wide control channel and a 100- μm -wide fluid channel. 100 \times 50 closing and opening data (not shown) are nearly identical to 50 \times 100 data. **(B)** Time response of a 100 μm by 100 μm by 10 μm RTV microvalve with 10-cm-long air tubing connected from the chip to a pneumatic valve. Two periods of digital control signal, actual air pressure at the end of the tubing, and valve opening are shown here. The pressure applied on the control line is 100 kPa, which is substantially higher than the ~ 40 kPa required to close the valve. Thus, when closing, the valve is pushed closed with a pressure 60 kPa greater than required. When opening, however, the valve is driven back to its rest position only by its own spring force (≤ 40 kPa). Thus, τ_{close} is expected to be smaller than τ_{open} . There is also a lag between the control signal and control pressure response, due to the limitations of the miniature valve used to control the pressure. Calling such lags t and the 1/e time constants τ , the values are $t_{\text{open}} = 3.63$ ms, $\tau_{\text{open}} = 1.88$ ms, $t_{\text{close}} = 2.15$ ms, and $\tau_{\text{close}} = 0.51$ ms. If 3τ each are allowed for opening and closing, the valve runs comfortably at 75 Hz when filled with aqueous solution (36). Valve opening was measured by fluorescence. The flow channel was filled with a solution of fluorescein isothiocyanate in buffer (pH ≥ 8), and the fluorescence of a square area occupying the center third of the channel was monitored on an epi-fluorescence microscope with a photomultiplier tube with a 10-kHz bandwidth. The pressure was monitored with a Wheatstone-bridge pressure sensor (SCC15GD2; Sensym, Milpitas, California) pressurized simultaneously with the control line through nearly identical pneumatic connections.

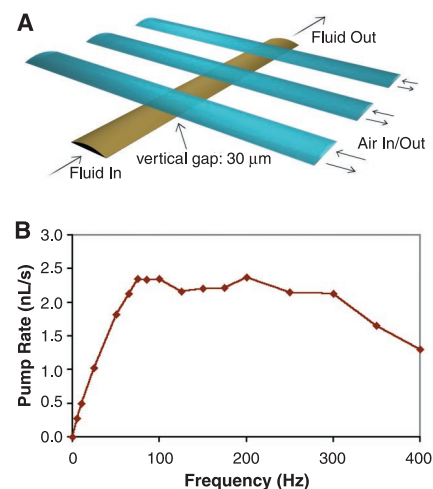


Fig. 4. (A) A 3D scale diagram of an elastomeric peristaltic pump. The channels are 100 μm wide and 10 μm high. Peristalsis was typically actuated by the pattern 101, 100, 110, 010, 011, 001, where 0 and 1 indicate "valve open" and "valve closed," respectively. This pattern is named the "120°" pattern, referring to the phase angle of actuation between the three valves. Other patterns are possible, including 90° and 60° patterns. The differences in pumping rate at a given frequency of pattern cycling were minimal. **(B)** Pumping rate of a peristaltic micropump versus various driving frequencies. Dimension of microvalves = 100 μm by 100 μm by 10 μm ; applied air pressure = 50 kPa.

with single-crystal silicon (~\$0.05/cm³ compared with ~\$2.5/cm³). Most important, it has a low Young's modulus, which allows actuation even of small area devices. Pneumatically actuated valves and pumps will be useful for a wide variety of fluidic manipulation for lab-on-a-chip applications. In the future, it should be possible to design electrically or magnetically actuated valves and pumps that can be used as implantable devices for clinical applications.

Note added in proof: After submission of this manuscript, we learned of related work by J. Anderson *et al.* in the Whitesides group at Harvard University.

References and Notes

1. L. M. Roylance and J. B. Angell, *IEEE Trans. Electron Devices* **ED-26**, 1911 (1979).
2. N. Yazdi, F. Ayazi, K. Najafi, *Proc. IEEE* **86**, 1640 (1998).
3. O. N. Tuftte, P. W. Chapman, D. Long, *J. Appl. Phys.* **33**, 3322 (1962).
4. L. Kuhn, E. Bassous, R. Lane, *IEEE Trans. Electron Devices* **ED-25**, 1257 (1978).
5. L. Y. Lin, E. L. Goldstein, R. W. Tkach, *IEEE J. Selected Top. Quantum Electron.* **5**, 4 (1999).
6. R. S. Muller and K. Y. Lau, *Proc. IEEE* **86**, 1705 (1998).
7. L. J. Hornbeck and W. E. Nelson, *OSA Tech. Dig. Ser.* **8**, 107 (1988).
8. D. J. Harrison *et al.*, *Science* **261**, 895 (1993).
9. S. C. Jacobson, R. Hergenroder, L. B. Koutny, J. M. Ramsey, *Anal. Chem.* **66**, 1114 (1994).
10. M. U. Kopp, A. J. de Mello, A. Manz, *Science* **280**, 1046 (1998).
11. S. Shoji, *Top. Curr. Chem.* **194**, 163 (1998).
12. P. Gravesen, J. Branebjerg, O. S. Jensen, *J. Micromech. Microeng.* **3**, 168 (1993).
13. L. Buchillot, E. Farnault, M. Hoummady, H. Fujita, *Jpn. J. Appl. Phys.* **2** **36**, L794 (1997).
14. Y. N. Xia *et al.*, *Science* **273**, 347 (1996).
15. Y. N. Xia and G. M. Whitesides, *Angew. Chem. Int. Ed. Engl.* **37**, 550 (1998).
16. C. S. Effenhauser, G. J. M. Bruin, A. Paulus, M. Ehrat, *Anal. Chem.* **69**, 3451 (1997).
17. E. Delamarche, A. Bernard, H. Schmid, B. Michel, H. Biebuyck, *Science* **276**, 779 (1997).
18. A. Y. Fu, C. Spence, A. Scherer, F. H. Arnold, S. R. Quake, *Nature Biotechnol.* **17**, 1109 (1999).
19. K. Hosokawa, T. Fujii, I. Endo, *Anal. Chem.* **71**, 4781 (1999).
20. D. C. Duffy, O. J. A. Schueller, S. T. Brittain, G. M. Whitesides, *J. Micromech. Microeng.* **9**, 211 (1999).
21. D. C. Duffy, J. C. McDonald, O. J. A. Schueller, G. M. Whitesides, *Anal. Chem.* **70**, 4974 (1998).
22. P. J. A. Kenis, R. F. Ismagilov, G. M. Whitesides, *Science* **285**, 83 (1999).
23. For multilayers, a thick layer was prepared as previously described; each thin layer was baked at 80°C for 20 min. The growing thick layer was assembled on each new thin layer and bonded by baking at 80°C for 20 min. Seven-layer devices have been produced by this method; no obvious limitations exist to limit the number of layers.
24. J. C. Lötters, W. Olthuis, P. H. Veltink, P. Bergveld, *J. Micromech. Microeng.* **7**, 145 (1997).
25. Conductive silicone was created by the addition of a fine carbon black (Vulcan XC72; Cabot, Billerica, MA) at 10% or higher concentration by weight. Conductivity increased with carbon black concentration from 5.6×10^{-16} to $\sim 5 \times 10^{-3}$ (ohm-cm)⁻¹. Magnetic silicone was created by the addition of iron powder (~1 μm particle size); up to 20% Fe by weight was added. For both conductive and magnetic silicones, multilayer bonding functioned normally.
26. K. Ikuta, K. Hirowatari, T. Ogata, in *Proceedings IEEE International MEMS 94 Conference* (IEEE, Piscataway, NJ, 1994), pp. 1-6.
27. R. B. M. Schasfoort, S. Schlautmann, J. Hendrikse, A. van den Berg, *Science* **286**, 942 (1999).

28. S. C. Jacobson, T. E. McKnight, J. M. Ramsey, *Anal. Chem.* **71**, 4455 (1999).
29. C. S. Effenhauser, G. J. M. Bruin, A. Paulus, *Electrophoresis* **18**, 2203 (1997).
30. M. Washizu, S. Suzuki, O. Kurosawa, T. Nishizaka, T. Shinohara, *IEEE Trans. Ind. Appl.* **30**, 835 (1994).
31. R. Pethig and G. H. Marx, *Trends Biotechnol.* **15**, 426 (1997).
32. R. Brechtel, W. Hoffmann, H. Rudiger, H. Watzig, *J. Chromatogr. A* **716**, 97 (1995).
33. C. A. Lucy and R. S. Underhill, *Anal. Chem.* **68**, 300 (1996).
34. The magnitude of flow (and even its direction) depends in a complicated fashion on ionic strength and type, the presence of surfactants, and the charge on the walls of the flow channel; furthermore, because electrolysis is taking place continuously, the capacity of buffer to resist pH changes is finite. Precise control of flow thus requires calibration for each new buffer or solute and can be difficult when the exact composition of a sample is not known in advance. Electroosmotic flow can also induce unwanted electrophoretic separation of molecules, creating demixing problems. Dielectrophoresis does not require electrolysis and therefore does not cause bubble formation but still suffers from sample and solvent sensitivity.
35. Each control channel was connected to the common port of a miniature three-way switch valve (LHDA1211111H; Lee Valve, Westbrook, CT), powered by a fast Zener-diode circuit and controlled by a

- digital data acquisition card (AT-DIO-32HS; National Instruments, Austin, TX). Regulated external pressure was provided to the normally closed port, allowing the control channel to be pressurized or vented to atmosphere by switching the miniature valve.
36. If one used another actuation method that did not suffer from opening and closing lag, this valve would run at ~375 Hz. The spring constant can be adjusted by changing the membrane thickness; this allows optimization for either fast opening or fast closing.
37. *E. coli* were pumped at 10 Hz through the channel. Samples of known volume were taken from the output well (pumped) and the input well (control), and serial dilutions of each were plated on Luria-Bertani agar plates and grown overnight at 37°C. Viability was assessed by counting colonies in the control and pumped samples and correcting for sample volumes and dilution.
38. J. Fahrenberg *et al.*, *J. Micromech. Microeng.* **5**, 77 (1995).
39. C. Goll *et al.*, *J. Micromech. Microeng.* **6**, 77 (1996).
40. X. Yang, C. Grosjean, Y. C. Tai, C. M. Ho, *Sensors Actuators A* **64**, 101 (1998).
41. A. M. Young, T. M. Bloomstein, S. T. Palmacci, *J. Biomech. Eng. Trans. ASME* **121**, 2 (1999).
42. This work was partially supported by NIH (NS-11756, DA-9121).

24 November 1999; accepted 14 February 2000

Chain Mobility in the Amorphous Region of Nylon 6 Observed under Active Uniaxial Deformation

Leslie S. Loo, Robert E. Cohen, Karen K. Gleason*

A specially designed solid-state deuterium nuclear magnetic resonance probe was used to examine the effect of uniaxial elongation on the chain mobility in the amorphous region of semicrystalline nylon 6. In measurements conducted near the glass transition temperature, there was measurable deformation-induced enhancement of the mobility of the amorphous chains up to the yield point. This enhanced mobility decayed once deformation was stopped. Enhanced mobility was not observed in deformation at room temperature. The mechanics of deformation can be explained by the Robertson model for glassy polymers near the glass transition temperature, which states that applied stress induces liquid-like behavior in the polymer chains.

Polymers are gradually replacing metals in many important engineering applications. Ongoing research seeks methodologies to design polymers with improved mechanical properties without sacrificing the advantages of low density and ease of processing. This task requires knowledge of deformation mechanisms, which are well understood in metals but less so in thermoplastic polymers. Various models have been proposed to account for plastic deformation in amorphous glassy polymers (1, 2). It is unclear whether such models can be used to

characterize the behavior in the amorphous region of semicrystalline polymers, such as nylon, because the presence of crystallites imposes topological constraints on the chains in the amorphous zones (3, 4).

Experimental elucidation of the deformation mechanism in polymers has focused on reconstructing the phenomenon on the basis of x-ray or nuclear magnetic resonance (NMR) measurements of the orientation or dynamics of the polymer after deformation has ceased, that is, in a "dead" polymer specimen (5, 6). Thus, any motions that may be activated by steady deformation or during yield would not be observed. Furthermore, the lack of long-range order in the amorphous regions of semicrystalline polymers precludes in-depth investigation by x-ray tech-

Department of Chemical Engineering and Center for Materials Science and Engineering, Massachusetts Institute of Technology, Cambridge, MA 02139, USA.

*To whom correspondence should be addressed. E-mail: kkgleas@mit.edu